Measuring walking and running dynamics using skin-mounted accelerometers

Surjo Dutta and David Friedman

University of Illinois at Urbana-Champaign, Dept. of Physics

Abstract—Asymmetries in the human gait are important in identifying and describing injuries or abnormalities of the lower limbs involved in walking or running. In the literature, many methods[7] have been used to measure the forces and accelerations experienced during human gait including various experiments involving accelerometers[6]. In this study, a series of accelerometers are attached to various parts of the lower limbs, and at the centre of mass (COM) of each subject. The 3-axis accelerations of these areas are measured and analysed to evaluate the utility of such accelerometers in identifying asymmetries and gait parameters. Using a peak-finding pedometer algorithm written in python, some gait parameters were successfully identified in ankle accelerations such as contact and propulsion acceleration magnitudes, and average step duration. Additionally, some asymmetries were identified in the gaits of two subjects demonstrating the feasibility of accelerometers for making such measurements.

I. Introduction

Stress injuries in lower limbs of runners are a frequent topic of study in kinesiology. Of these injuries, tibial stress fractures make up about 26-45%.[1] These injuries especially affect the performance of long distance runners, and increase post-workout recovery time.[2] Not only do such injuries lead to higher medical costs, they also take precious time away from an athlete's career, which is already known to be short.[3] As the number of runners in the US rises (from 38 million in 2006 to 56 million in 2017)[4] , it is becoming increasingly important to find a reliable and inexpensive method to conduct studies into the specifics of running and jogging techniques, and hopefully have a positive impact on the lives of these athletes, both monetarily and physically.

Studies like Brayne et al, 2018[5], Milner et al, 2007[6] and Lafortune et al, 1995[7] all attempted to measure the accelerations achieved in the tibial regions of runners and did so

with considerable precision. But each of these three studies used different methods to collect the data. Brayne et al. used a consumer-grade wireless accelerometer called RunScribe (RunScribe version 1, Scribe Labs, California, USA), which is a accelerometer-gyroscope sensor (MPU-9150) inertial measurement unit housed in a casing and attached directly to the

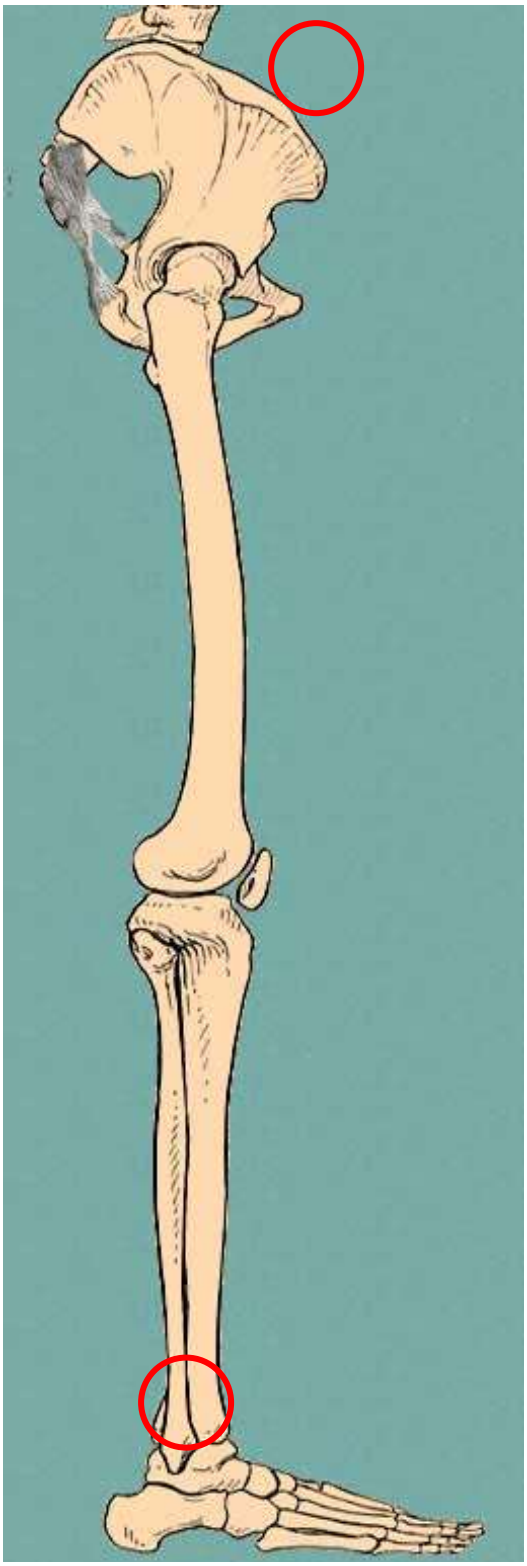

Figure 1 Diagram of the lower limbs and the accelerometer placement there on. The centre of mass accelerometer is typically placed such that the strap or belt holding it rests just above or on the hips. The ankle sensor is typically placed on the outside of the tibia, around the area indicated on the

skin of the subject using double-sided tape. The data from the sensor were sampled at 1kHz. Milner et al. on the other hand collected data at a lower sample rate 120Hz but used a less invasive method of a six camera Vicon 512 system (Oxford Metrics, Oxford, UK). Runners ran on treadmill fitted with a force-measuring platform while wearing shoes fitted with retro reflective tracking markers, to precisely track their movement. Lastly, Lafortune et al. used bone mounted transducers (BMTs) to do the job. Subjects had a triaxial accelerometer attached onto the tibia using a 4.7mm diameter Steinmann intracortical pin, which was inserted through a 3mm diameter pilot hole, right below the tibial plateau. Additionally, this was a comparative study which aimed to assess the value of skin mounted transducers (SMTs) to measure tibial shock, when compared to the bone mounted solution. So, alongside the BMT sensors, subjects were also fitted with SMTs and data from both sensors were collected simultaneously.

Although Lafortune et al. found a low correlation coefficient between SMT and BMT ($r = 0.55$) and on average a 2.1g greater peak tibial shock on the SMT, other studies[8] have found SMTs to report data with acceptable accuracy when the sensor mass is less than 3 grams. Additionally, SMTs are much less intrusive than BMTs, and less costly than the vision/videography based methods. For these reasons, we chose to mount our sensors directly on the skin of the subject.

II. Methods

The study consisted of two major components, the data acquisition system, and the post-processing of data.

The Device and Data Acquisition

Figure 2: The accelerometer-gyroscope sensor strapped to a subject's ankle

Our device was based on the Arduino Mega micro-controller, an inexpensive micro-controller used widely for data collection and other basic computation. The Arduino and the Arduino IDE (built on C++) provided the flexibility and speed we needed to collect and store data from the three accelerometer sensors we attached to the subject using Velcro straps. These sensors were 9-axis accelerometer-gyroscope-magnetometer combination sensors (LSM9DS1) which communicated with the main Arduino board through wired I2C[i] channels. Each sensor individually is capable of measuring accelerations of up to ±16*g*[ii] at a sample rate of about 1kHz, but with three sensors running simultaneously on one Arduino, and offloading the data to an SD card, the sample rate dropped to 110Hz, which is still an acceptable rate[8] for our purposes.

Along with the Arduino and the sensors, we needed a 9V battery connected to the device to power the system and to provide the subject some ease of mobility. The device also used an SD card writer to offload the data into an SD card. This process was the bottleneck for our data acquisition sample rate since data from three sensors, each consisting of 3-axis acceleration and 3-axis gyroscope was to be written to the SD for every sample, 110 times per second.

[i] I2C: A two-wire serial protocol used for communication between low power sensors and microcontrollers

[ii] Modes for ±2/4/8*g* were also available

The whole data acquisition device was kept in a tight runners' backpack to conserve the freedom of locomotion for the subject while jogging, walking, or running. We chose to use three sensors to maximise the information we could collect from various parts of the lower limbs and centre of mass of the subject while keeping the sample rate high enough for our data to high enough frequency and to avoid aliasing[iii] of our periodic running data. To provide flexibility for future studies of running related injuries, we tested our device by varying the placement of our sensors on the body. Data was collected with sensors placed on both ankles (attached to the skin), and at the approximate centre of mass of the subject (at about where the belt buckle would be).

Once the sensors were placed on the relevant sections of the lower limbs and/or on the COM of the subject, and the rest of the device was safely secured in the backpack, we began to take readings from the sensors. Each run started with the subject being asked to stand still and upright for 10 seconds, which was the calibration phase. This gave us enough data for post-processing to figure out the true z-axis and to calibrate our data points accordingly. After the calibration phase, the subject was asked to jog or walk at a steady pace for about a minute. Once the readings were taken, the data was downloaded onto a PC using the SD card for post-processing.

Post Processing

The analysis of experimental data was done offline in Python[iv] which reduced the complexity of the hardware and maximized the sample rate of the accelerometers. Limiting the data processing on the hardware means that all sensor calibration had to be done manually

[iii] Aliasing: The misidentification of a signal frequency, introducing distortion or error, occurs most commonly when rate of sampling of a periodic signal is too low
[iv] Python: A general-purpose programming language

in python. The coefficients for converting raw sensor data to units of *g* in the LSM9DS1 can be found in the accelerometer library for Arduino. The calibration algorithm calculates a bias for each accelerometer and gyroscope axis during an initial period of zero motion. These biases are then subtracted off the data values, leading to two axes that read approximately zero and one that reads approximately 1*g* (this axis must be chosen manually based off the actual orientation of the sensor). On average, this bias is calculated over around 600 data points.

The Scipy library contains the "butter" and "filtfilt" functions that can be used to implement high-pass, lowpass and bandpass Butterworth filters. These filters can be used to isolate the range of frequencies which walking or running gyroscope signals would likely occupy. The filtered gyroscope data can then be integrated to calculate an approximate angle. Using the roll, pitch and yaw angles calculated during integration the projection of the acceleration due to gravity on each axis of the accelerometer. This is then subtracted from the raw data in order to isolate only the accelerations from to the movement of the subject.

Once the data are read into python in the form of individual acceleration vector components, it is calibrated and the magnitude of the acceleration of each sensor is found. This acceleration magnitude data is then analysed using a pedometer algorithm.

The way our pedometer algorithm works is we first define a step and then partition the dataset into steps. Figure 3 and Figure 4 show the peaked nature of the acceleration magnitude data from ankle and centre of mass (COM) data. The pedometer algorithm starts to define steps by locating these peaks (or clusters of peaks). This is done by splitting the intervening data between the two peaks. These associations become the partitions of the data.

The partitions can then be combined to form a series of steps.

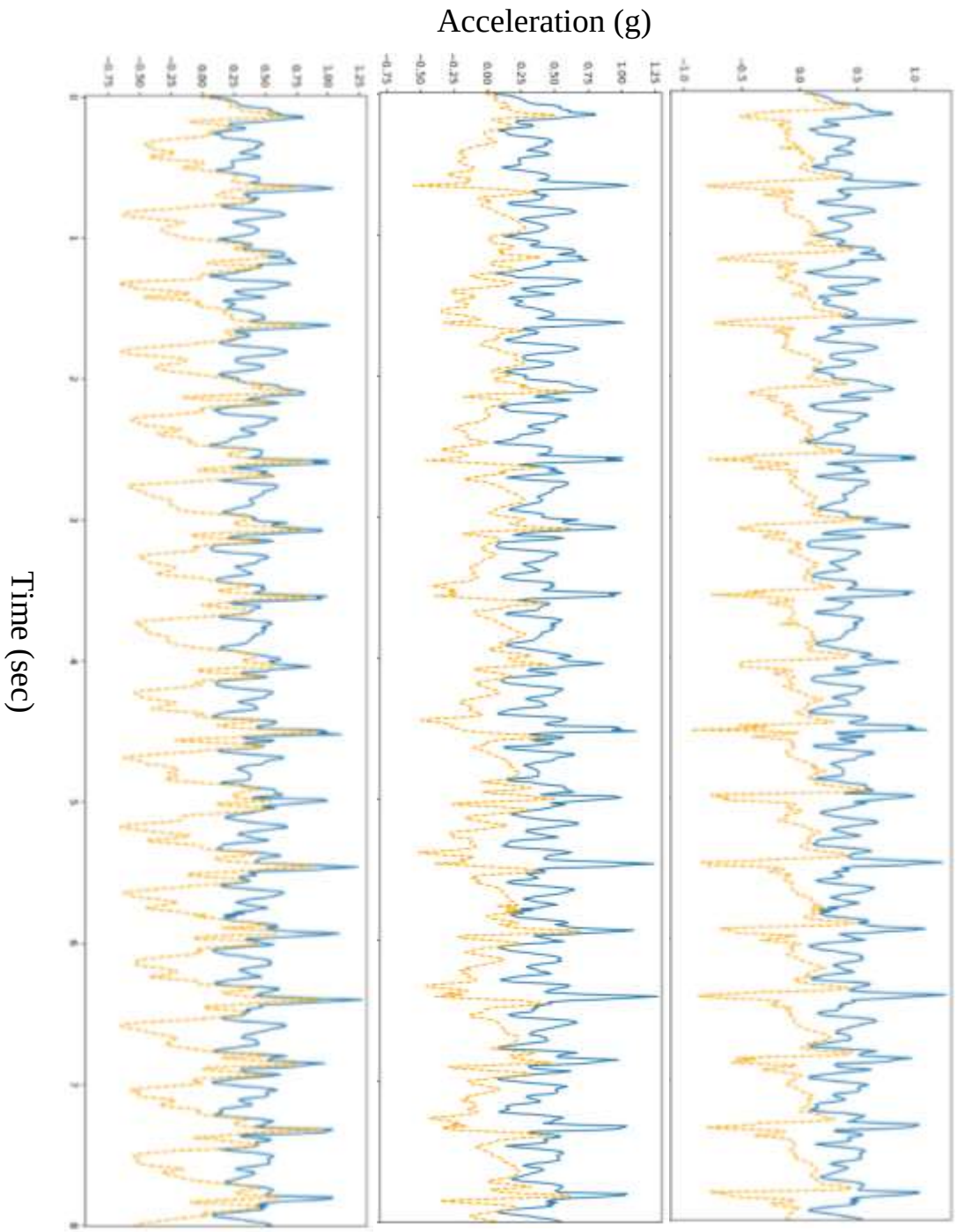

Figure 3.

a. Comparison of the acc. mag. with the forward-backwards acceleration of the sensor.

b. Comparison of the acc. mag. with the hip-movement (side to side) acceleration of the sensor.

c. Comparison of the acc. mag. with the up-down acceleration of the sensor.

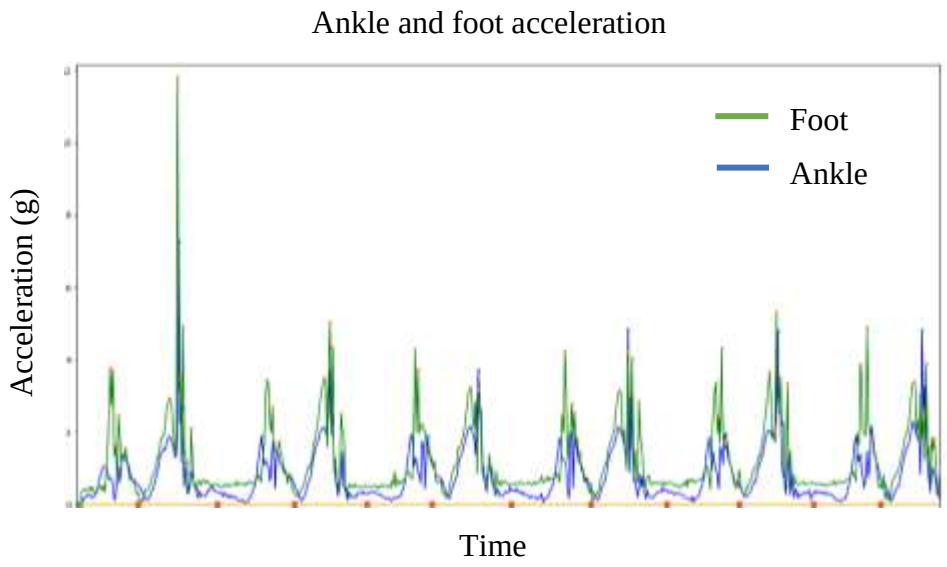

Figure 4.

Acceleration magnitude data from the foot and ankle sensors on one leg.

After the data has been partitioned into steps as described above, these partitions can be used to generate an average representation of the step data. The averaging algorithm generates an average profile of a step as defined by the partitions. Since the sizes of partitions can fluctuate, the features being averaged over can shift in time, generating some error. However, upon analysis, the fluctuations for most data points in the average representation are approximately gaussian and small, indicating that the partitioning algorithm works reasonably well.

Using the above described tools, this study will analyse the raw and averaged acceleration data gathered from walking and running subjects.

III. Results

Using three accelerometers, multiple parameters of a subject's gait could be measured. The data gathered during a particular test run was analyzed using the offline python tools described previously. Most of the analysis was done on the acceleration magnitudes which capture the dynamics from all three linear acceleration directions. The acceleration magnitude exhibits a clear periodic structure, particularly for the foot and ankle data; however, the individual directional components are necessary to fully understand the

structure of the acceleration magnitude. The centre of mass (COM) acceleration magnitude (Figure 1), for example, has a complicated, periodic peak structure. Unsurprisingly, the up-down motion (in the direction perpendicular to the floor) of the COM is approximately sinusoidal. It appears that the dominant acceleration peak comes from the upward acceleration of the COM. The smaller peaks come from the addition of the subsequent downward acceleration with other motions of the COM.

Understanding the acceleration magnitude data of the ankle and foot data gives a clearer picture of how the movement of both legs correlates to the COM data.

As seen in Figure 2 the foot and ankle data are sharply peaked and periodic as would be expected from an activity like walking. It should be noted that dominant double peak structure present can be misleading to the unfamiliar eye, as it only corresponds to steps from a single leg or foot as opposed to both. Comparing the ankle and foot acceleration magnitude signals shows that they are mostly similar in shape and magnitude on the larger peak but differ significantly on the smaller peak. In order to examine, in detail, the differences between a ‘step’ as observed by the foot and ankle accelerometers it is more useful to look at an average step representation.

Figure 5 shows the result of computing an average representation of a step yielding several useful pieces of information. Given a large enough data set, these average steps provide a practical way of estimating the duration of a step, the accelerations experienced during different phases, and the differences in these quantities across both legs. It should be noted that the uncertainty, while computed, has been omitted from Figure 5; it is large as the data set used to generate these averages contained very few steps. The largest uncertainties occur near the large peaks, as these shift significantly in time due to even small fluctuations in step duration.

Finally, the next data set was collected from both legs simultaneously as well as the centre of mass. Figure 5 shows the nature of the synchronization between the strides of this subject's legs. Each foot fall happens at about the half-way point of the push off the other

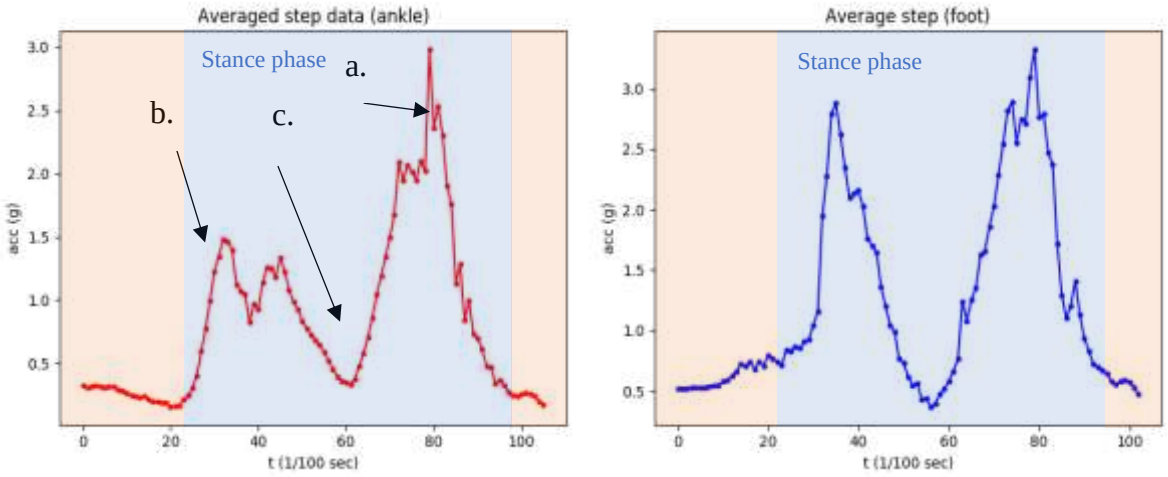

Figure 5. Using the pedometer algorithm, an individual step is defined. The acceleration magnitude data is then partitioned into the defined steps, and an average representation of a step is derived which is shown in these figures.

a. The propulsion phase of the stance phase of walking. The foot is pushing off the ground from the ball of the foot. The stride phase of each step follows this peak.

b. The contact phase of the stance phase of walking. The heel of the foot makes contact with the ground. We have not determined why this is double peaked, but we are convinced that the double peak is real.

c. The mid-step phase of the stance phase. Foot is fully planted on the ground.

foot. Once again, it is difficult to discern any quantitative differences in the acceleration data

from each leg without resorting to the aforementioned averaging algorithm. The following figures 6-9 show the averaged walking and running data from two subjects.

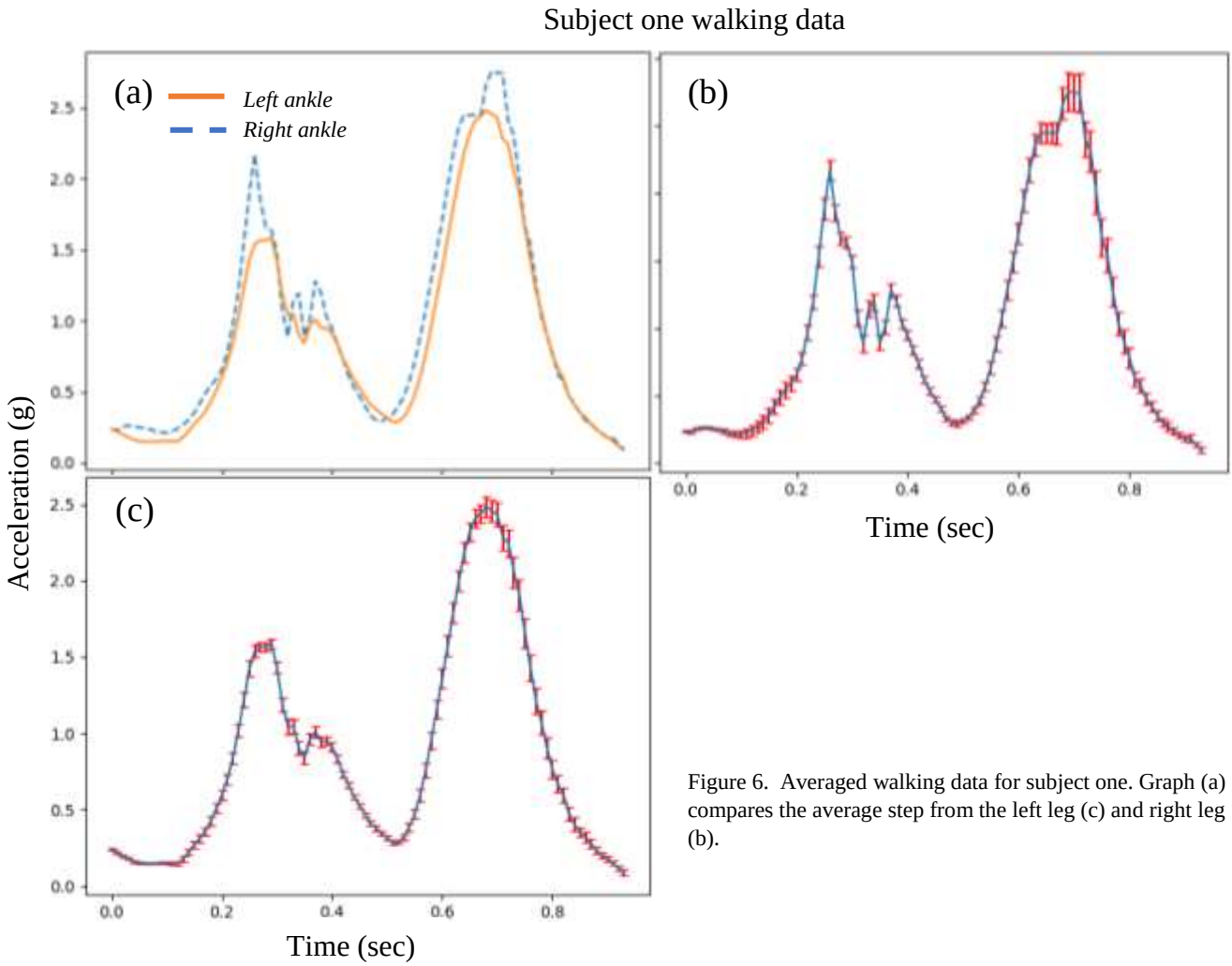

Figure 6. Averaged walking data for subject one. Graph (a) compares the average step from the left leg (c) and right leg (b).

Table 1	Right ankle	Left ankle
Step duration (ms):	926.0 +/- 7.8	927.9 +/- 6.9
Contact acceleration max (g):	2.172 +/- 0.075	1.567 +/- 0.032
Propulsion acceleration max (g):	2.757 +/- 0.143	2.483 +/- 0.068

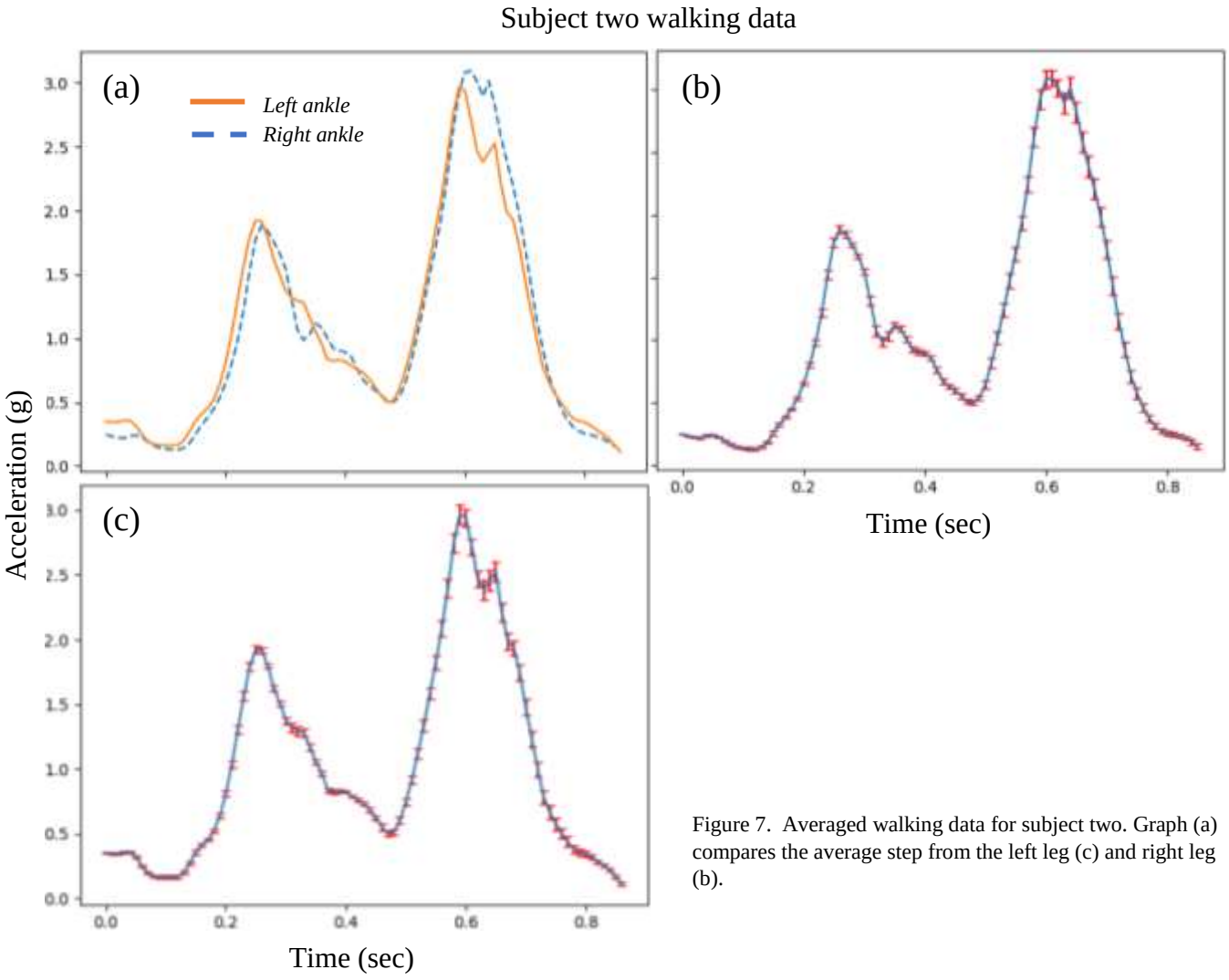

Figure 7. Averaged walking data for subject two. Graph (a) compares the average step from the left leg (c) and right leg (b).

Table 2	Right ankle	Left ankle
Step duration (ms):	856.4 +/- 4.51	856.5 +/- 4.50
Contact acceleration max (g):	1.870 +/- 0.032	1.911 +/- 0.031
Propulsion acceleration max (g):	3.283 +/- 0.065	2.976 +/- 0.073

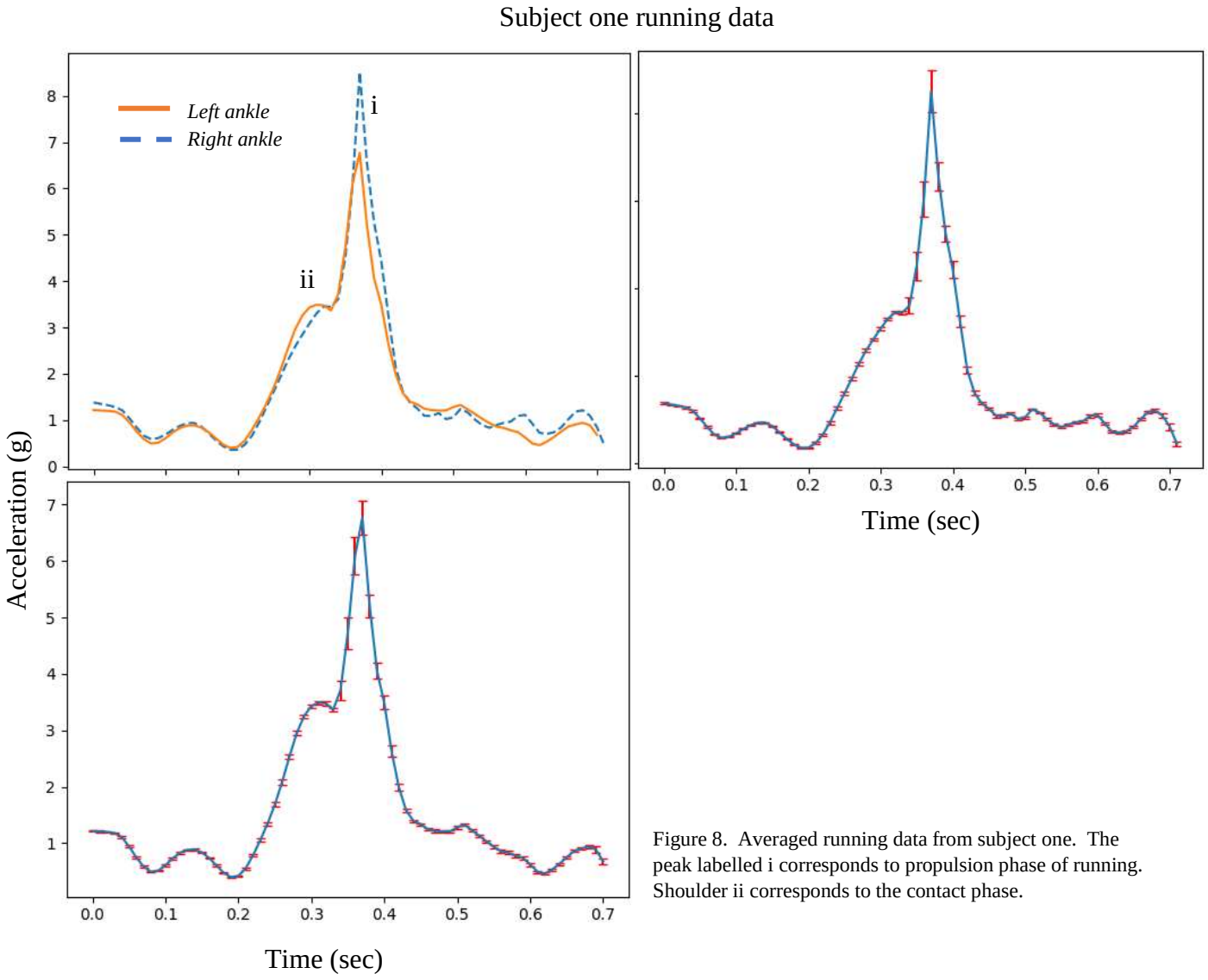

Figure 8. Averaged running data from subject one. The peak labelled i corresponds to propulsion phase of running. Shoulder ii corresponds to the contact phase.

Table 3	Right ankle	Left ankle
Step duration (ms):	711.2 +/- 58.1	708.3 +/- 55.3
Contact acceleration max (g):	N/A	3.488 +/- 0.032
Propulsion acceleration max (g):	8.511 +/- 0.482	6.769 +/- 0.339

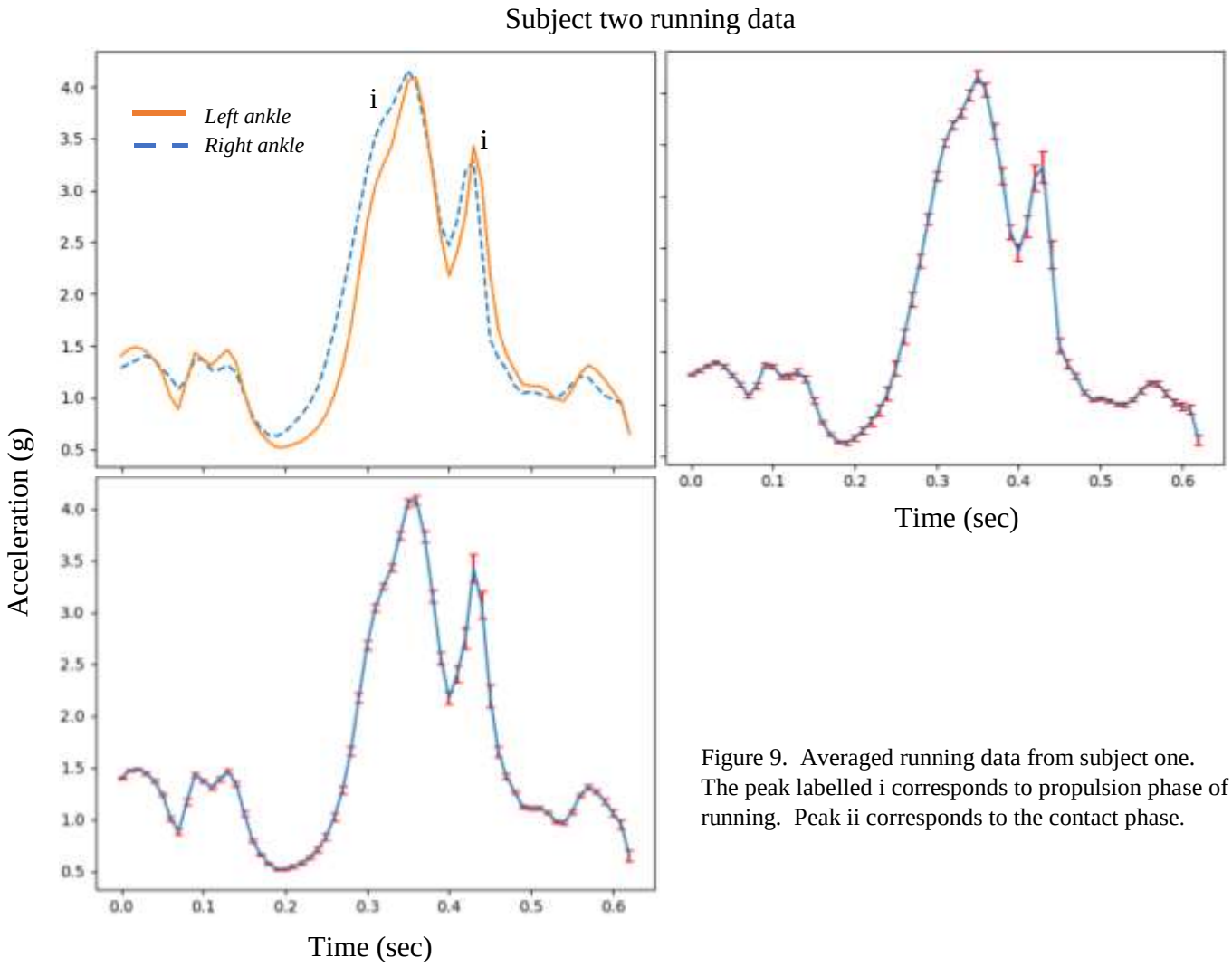

Figure 9. Averaged running data from subject one. The peak labelled i corresponds to propulsion phase of running. Peak ii corresponds to the contact phase.

Table 4	Right ankle	Left ankle
Step duration (ms):	623.2 +/- 48.1	623.4 +/- 48.0
Contact acceleration max (g):	4.156 +/- 0.063	4.089 +/- 0.043
Propulsion acceleration max (g):	3.284 +/- 0.148	3.427 +/- 0.131

IV. Error Analysis

There are several significant sources of error that should be discussed in detail. In particular, these errors mostly originate from the averaging and partitioning methods used in this study. The first issue arises due to the presence of significant perturbations (jolts, stumbles, or other irregularities observed) which can cause the partitioning procedure to behave in unexpected ways. Since partitions are read from their 'beginnings' to 'ends,' it is easy for a particular partition to be constructed backwards (ending where the others typically begin and vis versa). Once this reversal happens for one step it will continue to happen to all preceding steps. A single glitch in the data set can cause the resulting average to be a poor representation of a single step. The solution is to detect these glitches. In this study, these glitches are identified during an initial pass over the data set. The partitions generated from this first pass are checked for inconsistencies, the step reversal described above is easily identified using this method. The affected partitions are then corrected, resulting in a better average.

Another issue arises when the data are low resolution and are comprised of sharp peaks. Although the fluctuations in the duration of steps are not very significant compared to most features of the acceleration data, they are massive relative to sharp peaks. The result is that sharp peaks will be poorly represented in the average because their occurrence in time is uncertain compared to the duration of the peak feature. Combatting the loss of these peaks by increasing the threshold for acceptable peak values yields good results for data with a few very sharp features. However, for data with many close peaks of various amplitudes, increasing the threshold can actually generate worse representations. The tall peaks will tend to be represented better, while features that begin to fall below the threshold (on average) will quickly smear out. In these cases, it is better to leave the threshold low. Currently, such

threshold optimization tasks have to be done manually; however, optimization could possibly be automated by minimizing the variance of partition sizes and the variance of values at specific points like peaks or partition end points.

Finally, the slow and consistent change in step duration resulting from factors present in the subject's gait, while observable, are not accounted for in the averaging algorithm. In this study, data sets were short enough that subjects were able to maintain a very consistent pace for the duration of data collection. In general, subjects would perhaps inadvertently change their pace or gait during data collection. Such slow changes are outside of the scope of the averaging method and will likely cause it to perform poorly if those changes are too large.

The uncertainty associated with particular data points in the averages are generated using the following formula,

$$U = \frac{2\sigma}{\sqrt{N}} \tag{1.1}$$

where σ is the standard deviation of data points used to generate the averaged data point.

V. Discussion

Figure 10 **a.** Contact phase (stance). **b.** Propulsion phase (stance). **c-d.** Swing phase.

Figure 10 shows the general phases of the human gait: contact, propulsion, and swing phase. During the following discussion and in the results section these phases will be the standard interpretation of the averaged step data.

It is difficult to quantify the movement of joints or to exactly measure the motions of the subject with the accelerometers used in collecting the data presented in this project. Gravitational effects make the acceleration data too noisy to integrate without introducing significant drift. Unfortunately, without the visual aid position data would provide, the details of the accelerometer data quickly become difficult to interpret. However, as shown in the results section, some useful diagnostic parameters of a subject's walking gait can be extracted from a dataset of ankle or foot accelerations.

For example, it is clear from fig 6 (summarized in table 1) that the accelerations experienced by subject one's right leg are slightly but significantly greater than those experienced by the left leg; this asymmetry is also reflected in subject one's running data (fig. 7). The other parameter extracted, step duration, is approximately the same for the subject's left and right leg. Subject two also exhibits asymmetries in walking data (fig. 6) during the propulsion phase. The second subject's running acceleration data (fig. 8) is remarkably symmetric across left and right legs. It is currently unclear whether the afore mentioned asymmetries represent a pathology of the subject's gaits; however, for the purposes of this study the important point is that it is possible to measure asymmetries in leg accelerations using accelerometers.

It is worth describing how the phases gait can be seen in running data which appears characteristically different than walking data (see fig. 4 for a comprehensive explanation of how walking data is translated into gait phases). The most obvious difference between walking and running data is the number of distinct peaks. Walking data tends to have two

distinct peaks corresponding to contact and propulsion phases; running data appears to have a single strong peak with a small peak which often becomes a mere ‘shoulder.’ The apparent single peak and should structure could be viewed as a compression of the stance phase (propulsion and contact) and extension of the swing phase. Dr. Sylvia Ounpuu[9] presents an attempt to model this “transition” between walk and running where she appears to notice the same compression of gait during running. Subject one’s running gait as shown in fig. 8 exhibits a shoulder structure before a large sharp peak where as subject two’s (fig. 9) shows approximately the opposite pattern. The structure inversion most likely arises from the different dynamics of the ‘toe-strike’ gait used by subject one and ‘heel-strike’ gait of subject two. During the toe-strike gait, the toes of the subject land first during the contact phase and the foot the rotates the heel down to dissipate the subject’s downward momentum (the shoulder feature, fig. 8). The subject then launches from their toes into the swing phase (large peak, fig. 8). During the heel-strike gait (typical walking gait of most individuals), the subject lands on the heel of the foot during the contact phase and begins rolling forward (large peak in fig. 9). The subject then rolls onto their toes to launch forward during the propulsion phase (smaller peak, fig. 9). According to the data presented in figs 8 and 9, there are significant dynamic implications to the runner when choosing between heel and toe strikes. The most apparent difference is that the propulsion phase of the toe striker appears to generate more than double the acceleration of the heel-striker for a longer period of time. It should be noted that the phases of the running gait tend to be very short and sharp. The result is that the features are much lower resolution, and the averaging technique used to generate representations of an average step tends to smooth out sharp, low resolution peaks. This is particularly evident in the running data of subject two where the propulsion phase is very short and thus smeared out.

Another useful question is whether or not asymmetries can be spotted in the COM data which can be gathered with a single sensor. As can be seen in Figure 2, the COM acceleration magnitude data contains many more peaks than the ankle or foot data. These numerous peaks cause the COM acceleration mag. data to perform poorly in the pedometer

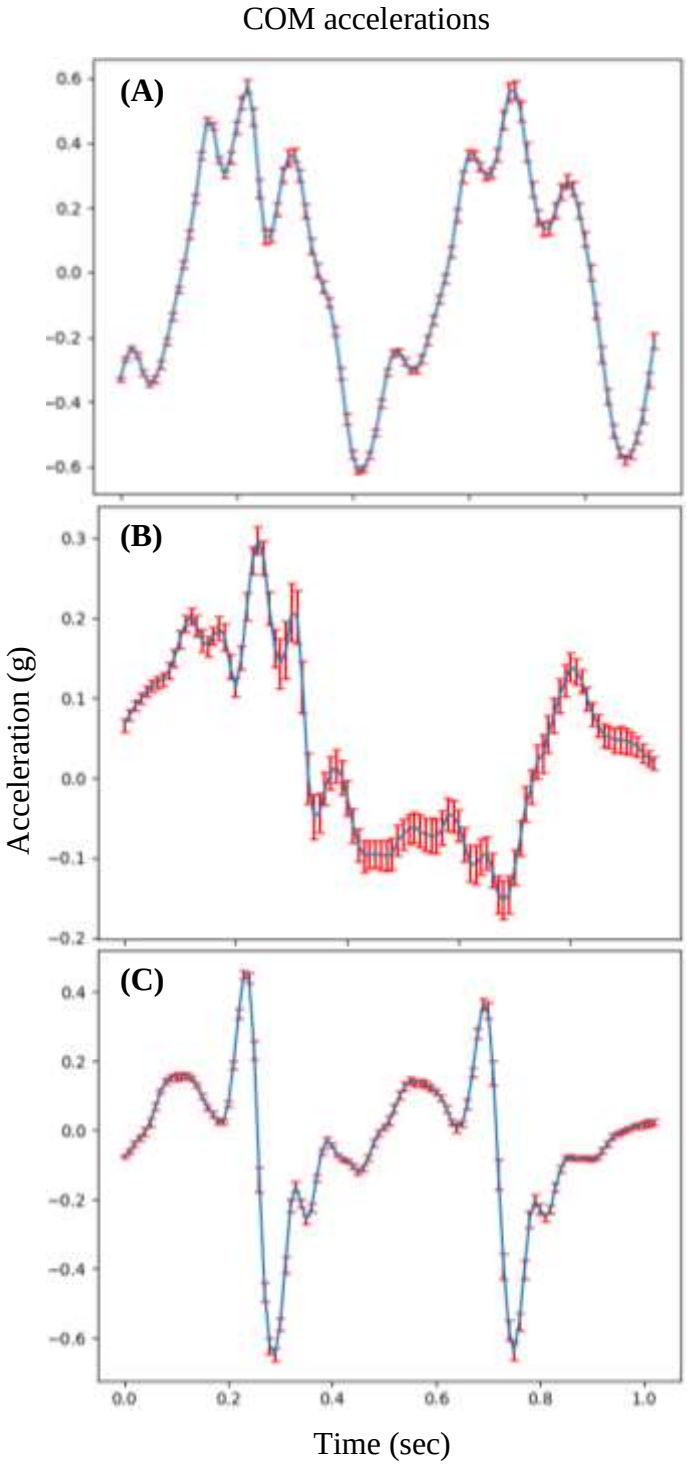

Figure 11. Averaged centre of mass acceleration data from subject one.

(A) vertical acceleration.

(B) acceleration due to hip motion.

(C) acceleration in the direction of motion of the subject.

Table 5		
Acc (g)	Peak 1	Peak 2
a.	-0.271 +/- 0.012	-0.262 +/- 0.011
b.	0.404 +/- 0.016	0.358 +/- 0.016
c.	0.576 +/- 0.022	0.540 +/- 0.027
d.	0.363 +/- 0.019	0.274 +/- 0.024
Duration (ms)	961.9 +/- 10.478	

algorithm. Instead it is easier to understand and analyse the individual components of the

COM acceleration vector.

Figure 11 shows the averages of the individual components of the COM acceleration. Each of these averaged profiles has approximately the same duration as a step (table 1). It should be noted, however, that the features do not exactly correspond in time to those shown in a single step. For example, the vertical component of the COM acceleration appears to be two periods of an approximately sinusoidal function. This vertical acceleration signal can be thought of as centered on one step signal from one leg; further, each series of peaks is also partly correlated with the propulsion and contact phases of the step signals before and after the centered step. The same applies to the other two acceleration signals. The multistep correlation associated with each peak is a simple consequence of how close each subsequent contact and propulsion phase is. In fact, fig. 5 shows that each foot contact begins approximately half-way through the propulsion phase of the other foot. The COM accelerations associated with hip-movement are small and difficult to interpret; they also have a relatively large uncertainty in their averaged form. For this subject, it may be more productive to ignore hip-movement and focus on the other components of the acceleration.

It is expected that changes in shape and magnitude of the vertical acceleration across adjacent periods would reveal asymmetries in the gait of the subject. Table 2 shows the magnitudes of the features identified in fig 12 for both peaks. Although all of these features appear in different magnitudes across both peaks, the differences are relatively small, with possibly the except of the feature labelled with a ‘d.’ On average, peak *d* differs significantly in magnitude and shape across the two periods. It seems that the accelerations surrounding peak *d* change more rapidly during the first period making the data look ‘stretched out’ compared to the second period.

As can be seen in Figure 13, the vertical accelerations of both feet are correlated with each vertical oscillation of the COM. It is plausible that the asymmetries seen in the vertical COM data are caused by those in the subject's gait.

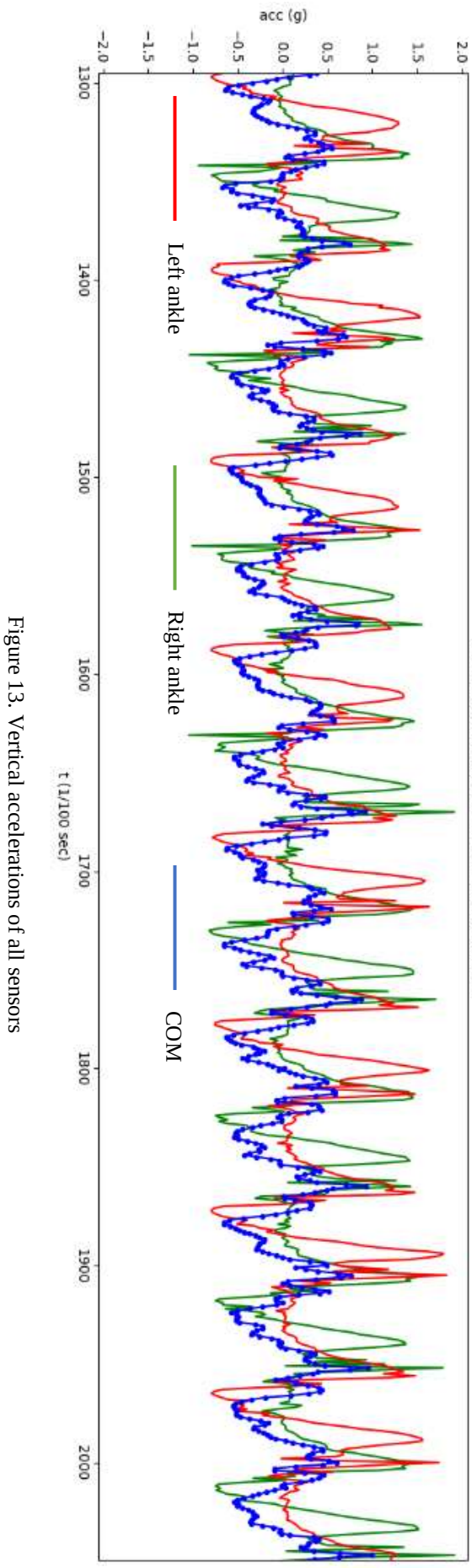

Figure 13. Vertical accelerations of all sensors

VI. Conclusion

In conducting this study, our main goal was to demonstrate a method to reliably collect relevant data from runners' bodies, specifically about the accelerations of their feet, heels, tibias and hip. We obtained accurate values of acceleration for each component of a step and showed how, using our method, one can collect raw data and process it to obtain a sensible graph which clearly shows the contact, mid-step and propulsion phases of a step, their magnitudes of acceleration, and the shape of the graph at each phase. Additionally, this method can also be used to measure tibial accelerations of subjects while walking.

As seen above, the method we used to collect the raw data using the Arduino and process it using Python is a feasible method which can be used by future studies. Examples of these include find relations between running related injuries and more specific components of running, like the running surface (treadmill vs track) or technique (heel strike vs forefoot running), or even use the data to predict/diagnose conditions in a subject, like limb length discrepancies or supination/pronation. With enough long-term data from healthy runners, runners with past injuries and runners who develop an injury over time, one can build a machine learning model which predicts the probability that a specific runner will develop an injury in the future if they keep using the technique they currently do. Apart from runners, this method could also be used to aid in rehabilitation of patients with lower limb injuries, offering an affordable alternative to current methods of detecting subtle variations between legs.

Works Cited

1. Bennell, Kim L., et al. "The Incidence and Distribution of Stress Fractures in Competitive Track and Field Athletes: A Twelve-Month Prospective Study." *The American Journal of Sports Medicine*, vol. 24, no. 2, Mar. 1996, pp. 211–217, doi:10.1177/036354659602400217.
2. Hreljac, Alan. "Impact and Overuse Injuries in Runners." *Medicine & Science in Sports & Exercise*, 1 May 2004, insights.ovid.com/crossref?an=00005768-200405000-00017.
3. Aschwanden, Christie. "Age Matters." *Runner's World*, 31 Aug. 2018, www.runnersworld.com/advanced/a20848096/age-matters-for-marathoning/.
4. "Running/Jogging Participants US 2006-2017 | Survey." *Statista*, 2017, www.statista.com/statistics/190303/running-participants-in-the-us-since-2006/.
5. Brayne, L., Barnes, A., Heller, B. et al. Sports Eng (2018) 21: 487. https://doi-org.proxy2.library.illinois.edu/10.1007/s12283-018-0271-4
6. Milner, Clare. "Are Knee Mechanics during Early Stance Related to Tibial Stress Fracture in Runners?" *Redirecting*, July 2017, doi.org/10.1016/j.clinbiomech.2007.03.003.
7. Lafortune, Mario. "Tibial Shock Measured with Bone and Skin Mounted Transducers." *Redirecting*, 1995, doi.org/10.1016/0021-9290(94)00150-3.
8. Chew, DK., Ngoh, K.JH., Gouwanda, D. et al. Sports Eng (2018) 21: 115. https://doi-org.proxy2.library.illinois.edu/10.1007/s12283-017-0255-9
9. Ounpuu, Sylvia. Clinics in Sports Medicine (1994). https://www.researchgate.net/publication/15394317_The_biomechanics_of_walking_and_running
10. Norman, Wesley. Lower Limb. http://www.wesnorman.com/llbones.htm